A diffusion model for light scattering in ejecta ⊕

J. A. Don Jayamanne ✉ ⓘ ; J.-R. Burie ⓘ ; O. Durand ⓘ ; R. Pierrat ⓘ ; R. Carminati ⓘ

Check for updates

View Online   Export Citation

Articles You May Be Interested In

Recovering particle velocity and size distributions in ejecta with photon Doppler velocimetry

J. Appl. Phys. (August 2024)

Characterization of ejecta in shock experiments with multiple light scattering

J. Appl. Phys. (February 2024)

Using ejecta measurement simulations to predict real-life results

Scilight (August 2024)

A diffusion model for light scattering in ejecta EP

View Online   Export Citation   CrossMark

J. A. Don Jayamanne,[1,2,a),b)] J.-R. Burie,[1,c)] O. Durand,[1] R. Pierrat,[2] and R. Carminati[2,3,d)]

AFFILIATIONS

[1] CEA DIF, Bruyères-le-Châtel, 91297 Arpajon Cedex, France
[2] Institut Langevin, ESPCI Paris, PSL University, CNRS, 75005 Paris, France
[3] Institut d'Optique Graduate School, Paris-Saclay University, 91127 Palaiseau, France

[a)] Author to whom correspondence should be addressed: j.don-jayamanne@exeter.ac.uk
[b)] Now at: Physics and Astronomy, University of Exeter, Exeter EX4 4QL, United Kingdom
[c)] Electronic mail: jean-rene.burie@cea.fr
[d)] Electronic mail: remi.carminati@espci.psl.eu

ABSTRACT

We derive a diffusion equation for light scattering from ejecta produced by extreme shocks on metallic samples. This model is easier to handle than a more conventional model based on the Radiative Transfer Equation (RTE) and is a relevant tool to analyze spectrograms obtained from Photon Doppler Velocimetry measurements in the deep multiple scattering regime. We also determine the limits of validity of the diffusive model compared to the RTE, based on a detailed analysis of various ejecta properties in configurations with increasing complexity.

I. INTRODUCTION

Ejection is a naturally occurring phenomenon when a metallic sample is subjected to an extreme shock. Through an explosive[1] or high intensity laser[2] solicitation, a shockwave can be released on one side of the sample with a typical shock pressure $P_s = 10 - 100$ GPa. Upon reaching the other side, called the free surface, the shockwave's interaction with the surface irregularities causes matter to partially melt, creating numerous expanding microjets. These microjets eventually fragment giving birth to a particle cloud called an ejecta.[3,4] A schematic representation of this microjetting mechanism is depicted from top to bottom in Fig. 1. Ejection has been extensively studied for the last fifty years[5] and is now understood as a limiting case of Richtmyer–Meshkov instabilities.[6,7] One of the current goal of ejecta study is to better characterize the particle cloud through its number density, size, or velocity distributions.

Photon Doppler Velocimetry (PDV) is one of the optical diagnostics used in this characterization effort. Initially developed to monitor particle velocities[8,9] in the single scattering regime, the PDV spectrogram of an experiment can be seen as a time-velocity cartography of the ejecta. Recently, we have shown that PDV spectrograms can also be interpreted in the multiple scattering regime even if they do not give direct access to the particle velocity distribution.[10,11] In this context and from a theoretical point of view, PDV spectrograms are solutions of a light transport model valid from the single scattering to the diffusive regime, and based on the Radiative Transfer Equation (RTE).[12,13]

Although the RTE is a highly relevant model for describing light propagation in a wide range of transport regimes, it remains difficult to manipulate. In practice, ejecta often have large optical thicknesses (typically on the order of 40). In such thick samples, a simplified model derived from the RTE and called the diffusion approximation[13,14] is commonly used to describe the propagation of light. This model is much simpler to handle, and in some cases even admits of analytical solutions. The purpose of this work consists in deriving a generalized diffusion equation valid for ejecta. The main idea is to adapt the standard derivation of the diffusion equation from the RTE by taking into account the specificities of ejecta (in particular, the statistical inhomogeneities and dynamic nature of the particle cloud). We will show how the diffusion approximation allows us to describe the PDV spectrograms much more easily and test the limits of this simplified model.
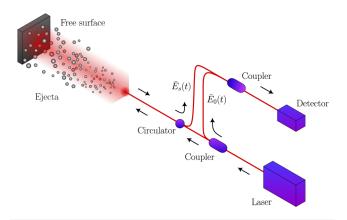
The paper is organized as follows. Section II is dedicated to the introduction of PDV, the associated spectrograms, and the theoretical model based on the RTE, valid from the single scattering to the deep multiple scattering regimes. In Sec. III, we perform the

FIG. 1. Illustration of the microjetting mechanism in a typical shock ejecta experiment. Upon reaching the machined free surface, the shock wave first comes into contact with the inwardly directed grooves. Under right angle conditions, the shock wave is reflected and the inward grooves become outward microjets. Due to the velocity gap between the jet-heads and the free surface, the microjets are stretched until surface tension is no longer sufficient to hold matter together and fragmentation begins. This results in the creation of a particle cloud, i.e., an ejecta.

FIG. 2. Schematic representation of a typical shock-loaded experiment with a PDV setup. The probe illuminates the ejecta and the free surface with a highly collimated laser beam (typical numerical aperture of $\theta_p = 4.2$ mrad and pupil size $\phi_p = 1.6$ mm). The backscattered field is collected by the probe acting as the measuring arm and interferes with the reference arm at the detector. The beating signal is registered with a high bandwidth oscilloscope before being analyzed.

diffusion approximation to obtain a diffusion equation for light propagation in ejecta. We compare the result to the standard diffusion equation and see especially how the displacement of the scatterers is effectively accounted for. Finally, a comprehensive study comparing the results given by the RTE and the diffusion equation for different dynamic media is reported in Sec. IV. To check the robustness of the diffusion model, we start from the simplest configuration and progressively increase the complexity to eventually treat the case of a real ejecta.

II. PHOTON DOPPLER VELOCIMETRY, SPECTROGRAMS, AND RADIATIVE TRANSFER

Photon Doppler Velocimetry is an interferometric technique,[8,9] where a probing laser field at frequency ω_0 is sent through an optical fiber toward a cloud of moving particles ejected from a free surface. As seen in Fig. 2, light is then scattered by this ejecta and slightly shifted in frequency due to the Doppler effect before being partially collected in reflection by the same fiber. This illumination and collection geometry was historically designed to probe the free surface velocity, but it is now also used to study ejecta. The collected field interferes at the detector with a reference field, at ω_0, resulting in a beating signal $\mathscr{I}(t)$ at the detector. This heterodyne detection ensures a good signal to noise ratio at optical frequencies.

This signal can be written as

$$\mathscr{I}(t) = 2\mathrm{Re}\left[\bar{\mathbf{E}}_s(\mathbf{r}, t) \cdot \bar{\mathbf{E}}_0^*(\mathbf{r}, t)\right], \tag{1}$$

with $\bar{\mathbf{E}}_s(\mathbf{r}, t)$ [respectively, $\bar{\mathbf{E}}_0(\mathbf{r}, t)$] being the analytic signal associated with the scattered (respectively, reference) field, $\mathbf{r}$ being the position of the probe, and the superscript $*$ denotes the complex conjugate.

In post-treatment, a short-term Fourier transform is applied defining the spectrogram $S(t, \Omega)$ as

$$S(t, \Omega) = \left|\int \mathscr{I}(\tau) w(\tau - t) \exp(i\Omega\tau)\, d\tau\right|^2 \tag{2}$$

where $w(t)$ is a gate function of typical width T_w such that $\int w(t)\, dt = T_w$. In Eq. (2), it can be easily shown that Ω corresponds to the Doppler shift experienced by light when propagating inside the ejecta. Time t corresponds to different instants in the ejecta's expansion. A spectrogram is, therefore, the result of a time-frequency analysis of the field scattered by the ejecta. Note that in the case of single backscattering, $\Omega = (4\pi)v/\lambda = 2k_0 v$, where v is the velocity of the particles and $k_0 = 2\pi/\lambda$ is the wavevector. In this particular case, a spectrogram can, therefore, be used to trace the particle velocity distribution as a function of time.

In the multiple scattering regime, however, interpretation is more complex and a more refined model is required to account for the spectrograms obtained experimentally. This model is derived in detail in Ref. 10, and we summarize here the main steps since they will serve as building blocks for obtaining the diffusion equation derived in Sec. III. We first need a quantity to describe light propagation in disordered media. A common one, also derived from a time–frequency analysis, is the specific intensity. It is defined as the

space and time Wigner transform of the field and is given by[13,15–17]

$$\delta(k - k_r)I(\mathbf{r}, \mathbf{u}, t, \omega)$$
$$= \int \left\langle \bar{E}\left(\mathbf{r} + \frac{\boldsymbol{\rho}}{2}, t + \frac{\tau}{2}\right) \bar{E}^*\left(\mathbf{r} - \frac{\boldsymbol{\rho}}{2}, t - \frac{\tau}{2}\right) \right\rangle$$
$$\exp(-i k\mathbf{u} \cdot \boldsymbol{\rho} + i\omega\tau) \, \mathrm{d}\boldsymbol{\rho} \, \mathrm{d}\tau, \quad (3)$$

where k_r is the real part of the effective wavevector in the scattering medium and $\langle \cdots \rangle$ denotes a statistical average over an ensemble of realizations of the disorder (i.e., the scatterers' position). The specific intensity $I(\mathbf{r}, \mathbf{u}, t, \omega)$ is defined from the field-field correlation function. In a radiometric picture, it can also be seen as a radiative flux at position $\mathbf{r}$, time t, and frequency ω, propagating along direction $\mathbf{u}$. The time τ plays the role of the correlation time. From various considerations on the time scales involved, we can show the spectrogram can be written in terms of the specific intensity and takes the form[10]

$$S(t, \Omega) \propto \int_{\theta_p} [I(\mathbf{r}, \mathbf{u}, t, \omega_0 + \Omega) + I(\mathbf{r}, \mathbf{u}, t, \omega_0 - \Omega)]\mathbf{u} \cdot \mathbf{n} \, \mathrm{d}\mathbf{u}, \quad (4)$$

where θ_p is the extremely narrow cone of collection of the probe around $\mathbf{n}$, the direction normal to the probe's pupil. Typically, we have $\theta_p = 4.2 \, \mathrm{mrad}$. $\mathrm{d}\mathbf{u}$ means integration over the solid angle. The key point here is that the spectrogram at time t and Doppler frequency Ω, which was initially introduced as a very specific time–frequency analysis of a beating signal, now appears as a relatively intuitive angular integral of the specific intensity at time t and frequencies $\omega_0 \pm \Omega$. This result makes the specific intensity the quantity of choice to describe spectrograms of ejecta.

Next, we need an equation governing the evolution of the specific intensity in ejecta. It is given by a generalized RTE,[10]

$$\left[\frac{1}{v_E(\mathbf{r}, t, \omega)}\frac{\partial}{\partial t} + \mathbf{u} \cdot \nabla_\mathbf{r} + \frac{1}{\ell_e(\mathbf{r}, t, \omega)}\right] I(\mathbf{r}, \mathbf{u}, t, \omega)$$
$$= \frac{1}{\ell_s(\mathbf{r}, t, \omega)} \int_{4\pi} p(\mathbf{r}, \mathbf{u}, \mathbf{u}', t, \omega, \omega') I(\mathbf{r}, \mathbf{u}', t, \omega') \, \mathrm{d}\mathbf{u}' \frac{\mathrm{d}\omega'}{2\pi}, \quad (5)$$

with v_E being the energy velocity, ℓ_e being the extinction mean free path, ℓ_s being the scattering mean free path, and p being the generalized phase function. In the phase function, $\mathbf{u}'$ and ω' are the incident direction and frequency, respectively, and $\mathbf{u}$ and ω are the scattered direction and frequency, respectively. Equation (5) takes into account the specificities of ejecta such as statistical inhomogeneity, polydispersity, and the motion of the particles in the ejecta.

We assume in the following that the ejecta is composed of spherical particles of different radii with an inhomogeneous number density depending on position and time. In this case, the extinction mean free path ℓ_e is given by

$$\frac{1}{\ell_e(\mathbf{r}, t, \omega)} = \int \rho(\mathbf{r}, t)\sigma_e(a, \omega)h(\mathbf{r}, t, a) \, \mathrm{d}a, \quad (6)$$

where $\rho(\mathbf{r}, t)$ is the number density of particles at position $\mathbf{r}$ and time t and $\sigma_e(a, \omega)$ is the extinction cross section of a particle with radius a at frequency ω. $h(\mathbf{r}, t, a)$ is the size distribution at position $\mathbf{r}$ and time t. The scattering mean free path ℓ_s and the generalized phase function p are defined as

$$\frac{1}{\ell_s(\mathbf{r}, t, \omega)}p(\mathbf{r}, \mathbf{u}, \mathbf{u}', t, \omega, \omega') = \int \rho(\mathbf{r}, t)\sigma_s(a, \omega)p(a, \mathbf{u} \cdot \mathbf{u}', \omega)$$
$$\times 2\pi\delta[\omega' - \omega - k_r(\mathbf{u}' - \mathbf{u}) \cdot \mathbf{v}]f(\mathbf{r}, t, a, \mathbf{v}) \, \mathrm{d}a \, \mathrm{d}\mathbf{v}, \quad (7)$$

where $\sigma_s(a, \omega)$ and $p(a, \mathbf{u} \cdot \mathbf{u}', \omega)$ are the scattering cross section and the phase function of a particle with radius a at frequency ω, respectively. The size-velocity distribution at position $\mathbf{r}$ and time t is given by $f(\mathbf{r}, t, a, \mathbf{v})$ with $h(\mathbf{r}, t, a) = \int f(\mathbf{r}, t, a, \mathbf{v}) \, \mathrm{d}\mathbf{v}$. We note that the phase function $p(a, \mathbf{u} \cdot \mathbf{u}', \omega)$ depends only on the dot product $\mathbf{u} \cdot \mathbf{u}'$ for a spherical particle. It is given by

$$p(a, \mathbf{u} \cdot \mathbf{u}', \omega) = \frac{1}{\sigma_s(a, \omega)}\frac{\mathrm{d}\sigma_s(a, \mathbf{u} \cdot \mathbf{u}', \omega)}{\mathrm{d}\mathbf{u}}, \quad (8)$$

where the differential scattering cross section $\mathrm{d}\sigma_s(a, \mathbf{u} \cdot \mathbf{u}', \omega)/\mathrm{d}\mathbf{u}$ corresponds to the radiation pattern. It is proportional to the part of radiated power coming from the incoming direction $\mathbf{u}'$ and scattered along the outgoing direction $\mathbf{u}$. Its integration over all possible directions gives the total scattering cross section. With this definition, the phase function is normalized as

$$\int_{4\pi} p(\mathbf{r}, \mathbf{u}, \mathbf{u}', t, \omega, \omega') \, \mathrm{d}\mathbf{u}' \frac{\mathrm{d}\omega'}{2\pi} = 1. \quad (9)$$

Thus, integrating Eq. (7) over $\mathbf{u}$, the scattering mean free path reads

$$\frac{1}{\ell_s(\mathbf{r}, t, \omega)} = \int \rho(\mathbf{r}, t)\sigma_s(a, \omega)h(\mathbf{r}, t, a) \, \mathrm{d}a. \quad (10)$$

We also introduce the absorption mean free path $\ell_a(\mathbf{r}, t)$ such that

$$\frac{1}{\ell_a(\mathbf{r}, t, \omega)} = \frac{1}{\ell_e(\mathbf{r}, t, \omega)} - \frac{1}{\ell_s(\mathbf{r}, t, \omega)}. \quad (11)$$

Finally, since we assume nonresonant scattering, the energy velocity v_E is given by $v_E(\mathbf{r}, t, \omega) = c/n_r(\mathbf{r}, t, \omega)$ where n_r is the real part of the effective optical index of the disordered medium (i.e., $k_r = n_r k_0$). The detailed physical interpretation of the generalized RTE as well as the derivation of the extinction mean free path, the scattering mean free path, and phase function expressions are discussed in greater detail in Ref. 10. In practice, the transport Eq. (5) can be solved numerically using a Monte Carlo scheme allowing to compute PDV spectrograms.[10]

In a standard experiment, we can assume that the optical properties of an ejecta are statistically invariant along the transverse directions and it is common to define the optical thickness b_s in an inhomogeneous ejecta as

$$b_s = \int_0^L \frac{\mathrm{d}z}{\ell_s(z)}, \quad (12)$$

where z denotes the position along the ejection direction and L the size of the ejecta along this direction. For the example treated in

Ref. [10], we found $b_s = 42$, which means that light interacts with the ejecta in the deep multiple scattering regime. For such optical thicknesses, it seems reasonable to investigate the possibility of using the diffusion approximation to describe the spectrograms, instead of the full RTE. This is the subject of Secs. III and IV.

III. DERIVATION OF A DIFFUSION EQUATION FOR LIGHT IN EJECTA

There are different ways to derive a diffusion equation starting from the RTE. One can introduce modes of the transport equation and define the diffusion mode as the mode surviving at the largest times and depths, a method also known as the singular eigenfunctions approach.[18,19] One can also perform a direct asymptotic analysis of the RTE at large scales.[13,20] Finally, an angular expansion over spherical harmonics of the specific intensity can also be introduced. A diffusion equation is then obtained by keeping only the first two terms, a method known as the P1 approximation.[14,21,22] Here, we will make use of the angular expansion approach (in the steps of the derivation in Ref. [14]) since it is the easiest to use in the case of statistical inhomogeneous and dynamic media such as ejecta. This idea of introducing a diffusion equation for dynamic media is not new. Several models have already been derived with different techniques[23–27] and have been used extensively to study light transport in colloids,[28] cold atomic gases,[29] or biological tissues.[30] We will draw inspiration out of all these works in the following. In particular, a fairly standard approach is to derive a diffusion equation for a static complex medium to determine the path-length probability density $P(s)$ and then include the dynamics of the medium afterwards. Here, we rigorously derive the diffusion equation from the RTE taking into account in the first place the scatterer displacements and all other important ejecta characteristics.

A. Transport equation in the time domain

We start by considering the quasi-homogeneous and inelastic RTE given in Eq. (5), in which we can neglect the time derivative since the illumination in the experiment is monochromatic (steady state) and the transit time for light within the scattering cloud remains short compared to the evolution time scale of the cloud (quasi-static approximation). Therefore, the time variable t becomes a parameter and we choose to drop it for the sake of simplicity. In addition, since the Doppler shifts around the illumination frequency ω_0 are small compared to the typical spectral variation scales of extinction and scattering cross sections, the frequency ω can be fixed at ω_0 in $\sigma_e(a, \omega)$, $\sigma_s(a, \omega)$ and in $p(a, \mathbf{u} \cdot \mathbf{u}', \omega)$ and we also drop this dependence for the sake of simplicity. Plugging the expression of the phase function, and with the simplifications above, the RTE in Eq. (5) can be rewritten as

$$\left[\mathbf{u} \cdot \nabla_{\mathbf{r}} + \frac{1}{\ell_e(\mathbf{r})}\right] I(\mathbf{r}, \mathbf{u}, \omega) = \rho(\mathbf{r}) \int \sigma_s(a) p(a, \mathbf{u} \cdot \mathbf{u}')$$
$$\times 2\pi \delta[\omega' - \omega - k_r(\mathbf{u}' - \mathbf{u}) \cdot \mathbf{v}] f(\mathbf{r}, a, \mathbf{v}) I(\mathbf{r}, \mathbf{u}', \omega') d\mathbf{u}' \frac{d\omega'}{2\pi} da \, d\mathbf{v}.$$
(13)

This form of the transport equation is not yet fully adapted to the derivation of a diffusion equation because the presence of an integral over frequencies needs to be handled correctly. To this end, we perform a Fourier transform with respect to $\omega - \omega_0$. This leads to

$$\left[\mathbf{u} \cdot \nabla_{\mathbf{r}} + \frac{1}{\ell_e(\mathbf{r})}\right] I(\mathbf{r}, \mathbf{u}, \tau)$$
$$= \rho(\mathbf{r}) \int_{4\pi} \sigma_s(a) p(a, \mathbf{u} \cdot \mathbf{u}') e^{ik_r(\mathbf{u}' - \mathbf{u}) \cdot \mathbf{v} \tau} f(\mathbf{r}, a, \mathbf{v}) I(\mathbf{r}, \mathbf{u}', \tau) d\mathbf{u}' da \, d\mathbf{v},$$
(14)

with

$$I(\mathbf{r}, \mathbf{u}, \tau) = \int I(\mathbf{r}, \mathbf{u}, \omega) e^{-i(\omega - \omega_0)\tau} \frac{d\omega}{2\pi},$$
(15)

ω_0 being a parameter in this expression. The factor $e^{ik_r(\mathbf{u}' - \mathbf{u}) \cdot \mathbf{v} \tau}$ appearing in Eq. (14) shows that inelastic scattering results in the appearance of a dephasing in the time domain. As the specific intensity $I(\mathbf{r}, \mathbf{u}, \tau)$ propagates through the medium, it accumulates phase shifts which at long correlation times eventually leads to full decorrelation.

The next step consists in defining effective scattering properties to make Eq. (14) similar to the standard RTE and then follow as closely as possible the steps of the standard derivation of the diffusion approximation presented in Ref. [14]. The effective scattering mean free path and phase function are, respectively, defined as

$$\frac{1}{\tilde{\ell}_s(\mathbf{r}, \mathbf{u}', \tau)} = \rho(\mathbf{r}) \int_{4\pi} \sigma_s(a) p(a, \mathbf{u} \cdot \mathbf{u}') e^{ik_r(\mathbf{u}' - \mathbf{u}) \cdot \mathbf{v} \tau} f(\mathbf{r}, a, \mathbf{v}) da \, d\mathbf{v} d\mathbf{u},$$
(16)

$$\tilde{p}(\mathbf{r}, \mathbf{u}, \mathbf{u}', \tau) = \tilde{\ell}_s(\mathbf{r}, \mathbf{u}', \tau) \rho(\mathbf{r}) \int \sigma_s(a) p(a, \mathbf{u} \cdot \mathbf{u}')$$
$$\times e^{ik_r(\mathbf{u}' - \mathbf{u}) \cdot \mathbf{v} \tau} f(\mathbf{r}, a, \mathbf{v}) da \, d\mathbf{v}.$$
(17)

We note that in the most general case, $\tilde{\ell}_s$ depends on the incoming direction $\mathbf{u}'$. However, it reduces to the standard scattering mean free path when $|\mathbf{v}| = 0$ (static scatterers) or when the statistical distribution of velocity is isotropic. With these definitions, Eq. (14) becomes

$$\left[\mathbf{u} \cdot \nabla_{\mathbf{r}} + \frac{1}{\ell_e(\mathbf{r})}\right] I(\mathbf{r}, \mathbf{u}, \tau) = \int_{4\pi} \frac{1}{\tilde{\ell}_s(\mathbf{r}, \mathbf{u}', \tau)} \tilde{p}(\mathbf{r}, \mathbf{u}, \mathbf{u}', \tau)$$
$$\times I(\mathbf{r}, \mathbf{u}', \tau) d\mathbf{u}'.$$
(18)

We now split the specific intensity into its ballistic I_b and diffuse I_d parts. Only the diffuse component will be driven by a diffusion equation, with the ballistic component appearing in a source term. As pictured in Fig. 3 and explained in greater detail in Sec. III D, in an ejecta geometry, the medium is illuminated along direction $-\mathbf{u}_z$ and the ballistic intensity gets backscattered by the free surface along $\mathbf{u}_z$. To account for both contributions, the

FIG. 3. Illustration of the two ballistic components existing in an ejecta illuminated by a plane wave in the direction $\mathbf{u}_0 = -\mathbf{u}_z$. The free surface is on the left.

specific intensity in the temporal domain reads

$$I(\mathbf{r}, \mathbf{u}, \tau) = I_d(\mathbf{r}, \mathbf{u}, \tau) + \delta(\mathbf{u} + \mathbf{u}_z)I_b^-(\mathbf{r}, \tau) + \delta(\mathbf{u} - \mathbf{u}_z)I_b^+(\mathbf{r}, \tau), \tag{19}$$

where I_b^- is the incident ballistic contribution propagation toward negative z and I_b^+ is the reflected ballistic contribution propagation toward positive z.

Inserting this decomposition into Eq. (18) yields a form of the latter with distributions and functions on either side of the equality. The distribution terms are then equalized to obtain a transport equation for $I_b^-(\mathbf{r}, \tau)$ and $I_b^+(\mathbf{r}, \tau)$ given by

$$\left[\pm \mathbf{u}_z \cdot \nabla_{\mathbf{r}} + \frac{1}{\ell_e(\mathbf{r})} \right] I_b^{\pm}(\mathbf{r}, \tau) = 0. \tag{20}$$

In a similar way, function terms are equalized to obtain a transport equation for the diffuse intensity $I_d(\mathbf{r}, \mathbf{u}, \tau)$, which reads

$$\left[\mathbf{u} \cdot \nabla_{\mathbf{r}} + \frac{1}{\ell_e(\mathbf{r})} \right] I_d(\mathbf{r}, \mathbf{u}, \tau)$$
$$= \frac{1}{\tilde{\ell}_s(\mathbf{r}, -\mathbf{u}_z, \tau)} \tilde{p}(\mathbf{r}, \mathbf{u}, -\mathbf{u}_z, \tau) I_b^-(\mathbf{r}, \tau)$$
$$+ \frac{1}{\tilde{\ell}_s(\mathbf{r}, \mathbf{u}_z, \tau)} \tilde{p}(\mathbf{r}, \mathbf{u}, \mathbf{u}_z, \tau) I_b^+(\mathbf{r}, \tau)$$
$$+ \int_{4\pi} \frac{1}{\tilde{\ell}_s(\mathbf{r}, \mathbf{u}', \tau)} \tilde{p}(\mathbf{r}, \mathbf{u}, \mathbf{u}', \tau) I_d(\mathbf{r}, \mathbf{u}', \tau) \, d\mathbf{u}'. \tag{21}$$

Since the ballistic terms I_b^- and I_b^+ act as a source terms for I_d, solving Eq. (20) will be a prerequisite to solve the final diffusion equation.

B. Moments of the transport equation and P1 approximation

A diffusion equation is usually obtained by means of an energy balance and Fick's or Fourier's law. The first is obtained from the zero-order angular moment of the RTE. The second is derived from the first-order angular moment. This subsection is dedicated to obtaining these two equations under the P1

approximation. The zero-order moment of the RTE is obtained by integrating Eq. (21) over the direction $\mathbf{u}$. This leads to

$$\nabla_{\mathbf{r}} \cdot \mathbf{q}_d(\mathbf{r}, \tau) + \frac{v_E(\mathbf{r})}{\ell_e(\mathbf{r})} u_d(\mathbf{r}, \tau) = \int \frac{1}{\tilde{\ell}_s(\mathbf{r}, \mathbf{u}', \tau)} I_d(\mathbf{r}, \mathbf{u}', \tau) \, d\mathbf{u}' + S_0(\mathbf{r}, \tau), \tag{22}$$

with the diffusive energy current defined as

$$\mathbf{q}_d(\mathbf{r}, \tau) = \int_{4\pi} I_d(\mathbf{r}, \mathbf{u}, \tau) \mathbf{u} \, d\mathbf{u}, \tag{23}$$

the diffuse energy density defined as

$$u_d(\mathbf{r}, \tau) = \frac{1}{v_E(\mathbf{r})} \int_{4\pi} I_d(\mathbf{r}, \mathbf{u}, \tau) \, d\mathbf{u}, \tag{24}$$

and the source term defined as

$$S_0(\mathbf{r}, \tau) = \frac{1}{\tilde{\ell}_s(\mathbf{r}, -\mathbf{u}_z, \tau)} I_b^-(\mathbf{r}, \tau) + \frac{1}{\tilde{\ell}_s(\mathbf{r}, \mathbf{u}_z, \tau)} I_b^+(\mathbf{r}, \tau). \tag{25}$$

For static disorder (i.e., statistical realizations of the medium where the particles are assumed to have a null velocity), Eq. (22) reduces to a local energy balance law involving only u_d and $\mathbf{q}_d$. The situation is different here due to the angular dependence of the effective scattering mean free path. To get closer to an energy balance, which is a prerequisite for obtaining a diffusion equation, it is necessary to introduce the P1 approximation. It consists in considering that at large depths and long times (the meaning of large will be made quantitative later), the specific intensity is almost isotropic. Note that this is achievable only if absorption is weak compared to scattering. For ejecta, we typically have $\ell_a/\ell_s \approx 10$ (see Ref. 31). The specific intensity can be written as a first-order expansion in spherical harmonics and takes the form that reads

$$I_d(\mathbf{r}, \mathbf{u}, \tau) = \frac{v_E(\mathbf{r})}{4\pi} u_d(\mathbf{r}, \tau) + \frac{3}{4\pi} \mathbf{q}_d(\mathbf{r}, \tau) \cdot \mathbf{u}. \tag{26}$$

We note that the prefactors of each order are fully determined by Eqs. (23) and (24).[14,21,22]

Plugging this approximation in Eq. (22), the zero-order moment of the RTE then reads

$$\nabla_{\mathbf{r}} \cdot \mathbf{q}_d(\mathbf{r}, \tau) + \frac{v_E(\mathbf{r})}{\ell_e(\mathbf{r})} u_d(\mathbf{r}, \tau) = v_E(\mathbf{r}) M_0(\mathbf{r}, \tau) u_d(\mathbf{r}, \tau)$$
$$+ 3\mathbf{M}_1(\mathbf{r}, \tau) \cdot \mathbf{q}_d(\mathbf{r}, \tau) + S_0(\mathbf{r}, \tau), \tag{27}$$

with

$$M_0(\mathbf{r}, \tau) = \frac{1}{4\pi} \int \frac{1}{\tilde{\ell}_s(\mathbf{r}, \mathbf{u}', \tau)} \, d\mathbf{u}', \tag{28}$$

$$\mathbf{M}_1(\mathbf{r}, \tau) = \frac{1}{4\pi} \int \frac{1}{\tilde{\ell}_s(\mathbf{r}, \mathbf{u}', \tau)} \mathbf{u}' d\mathbf{u}', \tag{29}$$

the first two angular moments of $1/\tilde{\ell}_s$. While in the regular derivation of the diffusion equation $M_0 = 1/\ell_s$, the presence of $\mathbf{M}_1(\mathbf{r}, \tau)$ is specific to dynamic media with anisotropic velocity distribution.

Likewise, to obtain the first-order angular moment of the transport equation, we multiply Eq. (21) by $\mathbf{u}$ and integrate over $\mathbf{u}$. We obtain

$$\int \mathbf{u} \cdot \nabla_\mathbf{r} I_d(\mathbf{r}, \mathbf{u}, \tau)\mathbf{u}\,\mathrm{d}\mathbf{u} + \frac{1}{\ell_e(\mathbf{r})}\mathbf{q}_d(\mathbf{r}, \tau)$$
$$= \int \frac{1}{\tilde{\ell}_s(\mathbf{r}, \mathbf{u}', \tau)}\tilde{p}(\mathbf{r}, \mathbf{u}, \mathbf{u}', \tau)I_d(\mathbf{r}, \mathbf{u}', \tau)\mathbf{u}\,\mathrm{d}\mathbf{u}'\,\mathrm{d}\mathbf{u} + \mathbf{S}_1(\mathbf{r}, \tau), \quad (30)$$

with the source term

$$\mathbf{S}_1(\mathbf{r}, \tau) = \frac{1}{\tilde{\ell}_s(\mathbf{r}, -\mathbf{u}_z, \tau)}I_b^-(\mathbf{r}, \tau)\int \tilde{p}(\mathbf{r}, \mathbf{u}, -\mathbf{u}_z, \tau)\mathbf{u}\,\mathrm{d}\mathbf{u}$$
$$+ \frac{1}{\tilde{\ell}_s(\mathbf{r}, \mathbf{u}_z, \tau)}I_b^+(\mathbf{r}, \tau)\int \tilde{p}(\mathbf{r}, \mathbf{u}, \mathbf{u}_z, \tau)\mathbf{u}\,\mathrm{d}\mathbf{u}. \quad (31)$$

As in the usual derivation,[14] we define the (effective) anisotropy factor as

$$\tilde{g}(\mathbf{r}, \mathbf{u}', \tau) = \int \tilde{p}(\mathbf{r}, \mathbf{u}, \mathbf{u}', \tau)(\mathbf{u} \cdot \mathbf{u}')\,\mathrm{d}\mathbf{u}, \quad (32)$$

which allows us to rewrite the first term in the right-hand side of Eq. (30) as

$$\int \frac{1}{\tilde{\ell}_s(\mathbf{r}, \mathbf{u}', \tau)}\tilde{p}(\mathbf{r}, \mathbf{u}, \mathbf{u}', \tau)I_d(\mathbf{r}, \mathbf{u}', \tau)\mathbf{u}\,\mathrm{d}\mathbf{u}'\,\mathrm{d}\mathbf{u}$$
$$= \int \frac{\tilde{g}(\mathbf{r}, \mathbf{u}', \tau)}{\tilde{\ell}_s(\mathbf{r}, \mathbf{u}', \tau)}I_d(\mathbf{r}, \mathbf{u}', \tau)\mathbf{u}'\,\mathrm{d}\mathbf{u}'. \quad (33)$$

Plugging again the P1 approximation given by Eq. (26) in this relation, we obtain

$$\int \frac{\tilde{g}(\mathbf{r}, \mathbf{u}', \tau)}{\tilde{\ell}_s(\mathbf{r}, \mathbf{u}', \tau)}I_d(\mathbf{r}, \mathbf{u}', \tau)\mathbf{u}'\,\mathrm{d}\mathbf{u}'$$
$$= v_E(\mathbf{r})u_d(\mathbf{r}, \tau)\mathbf{G}_1(\mathbf{r}, \tau) + \overleftrightarrow{\mathbf{G}}_2(\mathbf{r}, \tau)\mathbf{q}_d(\mathbf{r}, \tau), \quad (34)$$

with

$$\mathbf{G}_1(\mathbf{r}, \tau) = \int \frac{\tilde{g}(\mathbf{r}, \mathbf{u}', \tau)}{4\pi\tilde{\ell}_s(\mathbf{r}, \mathbf{u}', \tau)}\mathbf{u}'\,\mathrm{d}\mathbf{u}', \quad (35)$$

$$\overleftrightarrow{\mathbf{G}}_2(\mathbf{r}, \tau) = 3\int \frac{\tilde{g}(\mathbf{r}, \mathbf{u}', \tau)}{4\pi\tilde{\ell}_s(\mathbf{r}, \mathbf{u}', \tau)}(\mathbf{u}' \otimes \mathbf{u}')\,\mathrm{d}\mathbf{u}'. \quad (36)$$

Again, $\mathbf{G}_1$ would not appear in the standard derivation of the diffusion approximation and $\overleftrightarrow{\mathbf{G}}_2$ would be simply given by $g/\ell_s \overleftrightarrow{\mathbf{I}}$ with $\overleftrightarrow{\mathbf{I}}$ being the unit second-rank tensor.

In the following, we assume that the energy velocity v_E depends weakly on the position $\mathbf{r}$ since it is given by the real part of the effective refractive index n_r, which can be approximated by

the air refractive index (i.e. $n_r \approx 1$) in a dilute medium such as an ejecta. Therefore, we can assume $\nabla_\mathbf{r} v_E(\mathbf{r}) \approx 0$ and using again the P1 approximation, it is straightforward to show that the first term in the left-hand side of Eq. (30) can be rewritten as

$$\int \mathbf{u} \cdot \nabla_\mathbf{r} I_d(\mathbf{r}, \mathbf{u}, \tau)\mathbf{u}\,\mathrm{d}\mathbf{u} = \frac{v_E(\mathbf{r})}{3}\nabla_\mathbf{r} u_d(\mathbf{r}, \tau). \quad (37)$$

Finally, the first moment of the RTE, Eq. (30), leads to

$$\frac{v_E(\mathbf{r})}{3}\nabla_\mathbf{r} u_d(\mathbf{r}, \tau) + \frac{1}{\ell_e(\mathbf{r})}\mathbf{q}_d(\mathbf{r}, \tau) = \mathbf{G}_1(\mathbf{r}, \tau)v_E(\mathbf{r})u_d(\mathbf{r}, \tau)$$
$$\overleftrightarrow{\mathbf{G}}_2(\mathbf{r}, \tau)\mathbf{q}_d(\mathbf{r}, \tau) + \mathbf{S}_1(\mathbf{r}, \tau). \quad (38)$$

This equation can be cast in a form similar to Fick's law

$$\mathbf{q}_d(\mathbf{r}, \tau) = \overleftrightarrow{\mathbf{D}}(\mathbf{r}, \tau)\left[-\nabla_\mathbf{r} u_d(\mathbf{r}, \tau)\right.$$
$$\left. + 3\mathbf{G}_1(\mathbf{r}, \tau)u_d(\mathbf{r}, \tau) + \frac{3}{v_E(\mathbf{r})}\mathbf{S}_1(\mathbf{r}, \tau)\right], \quad (39)$$

with the diffusion tensor

$$\overleftrightarrow{\mathbf{D}}(\mathbf{r}, \tau) = \frac{v_E(\mathbf{r})}{3}\left[\frac{\overleftrightarrow{\mathbf{I}}}{\ell_e(\mathbf{r})} - \overleftrightarrow{\mathbf{G}}_2(\mathbf{r}, \tau)\right]^{-1}. \quad (40)$$

C. Diffusion equation

The features of ejecta, such as statistical inhomogeneities, anisotropy, and particle motion, greatly complicate the equations with the emergence of new quantities such as $\mathbf{M}_1(\mathbf{r}, \tau)$ and $\mathbf{G}_1(\mathbf{r}, \tau)$ and the dependence on τ in many of them. Usually, the temporal decorrelation of the beam appears in the model as an effective absorption term.[23] This effective absorption is very likely to be the dominant contribution here as well, and in the following we choose to neglect the τ dependence in all parameters except in the effective absorption, i.e., the term $1/\ell_e - M_0$ in Eq. (27). In practice, it means replacing $\tilde{\ell}_s$ and $\tilde{p}$ introduced in Eqs. (16) and (17) by, respectively, ℓ_s and p. The validity of this approximation will be checked in Sec. IV by comparison to a full treatment of the problem with the RTE. Under this assumption, the source terms and the angular moments of the effective scattering mean free path can be simplified. We find that

$$S_0(\mathbf{r}, \tau) = \frac{1}{\tilde{\ell}_s(\mathbf{r}, -\mathbf{u}_z, \tau)}I_b^-(\mathbf{r}, \tau) + \frac{1}{\tilde{\ell}_s(\mathbf{r}, \mathbf{u}_z, \tau)}I_b^+(\mathbf{r}, \tau)$$
$$\approx \frac{I_b^-(\mathbf{r}, \tau) + I_b^+(\mathbf{r}, \tau)}{\ell_s(\mathbf{r})}, \quad (41)$$

05 December 2025 08:18:02

$$\mathbf{S}_1(\mathbf{r}, \tau) = \frac{I_b^-(\mathbf{r}, \tau)}{\tilde{\ell}_s(\mathbf{r}, -\mathbf{u}_z, \tau)} \int \tilde{p}(\mathbf{r}, \mathbf{u}, -\mathbf{u}_z, \tau) \mathbf{u}\, d\mathbf{u}$$
$$+ \frac{I_b^+(\mathbf{r}, \tau)}{\tilde{\ell}_s(\mathbf{r}, \mathbf{u}_z, \tau)} \int \tilde{p}(\mathbf{r}, \mathbf{u}, \mathbf{u}_z, \tau) \mathbf{u}\, d\mathbf{u}$$
$$\approx g(\mathbf{r}) \frac{I_b^+(\mathbf{r}, \tau) - I_b^-(\mathbf{r}, \tau)}{\ell_s(\mathbf{r})} \mathbf{u}_z, \tag{42}$$

$$\mathbf{M}_1(\mathbf{r}, \tau) = \int \frac{\mathbf{u}'}{4\pi \tilde{\ell}_s(\mathbf{r}, \mathbf{u}', \tau)}\, d\mathbf{u}' \approx \mathbf{0}, \tag{43}$$

$$\mathbf{G}_1(\mathbf{r}, \tau) = \int \frac{\tilde{g}(\mathbf{r}, \mathbf{u}', \tau)}{4\pi \tilde{\ell}_s(\mathbf{r}, \mathbf{u}', \tau)} \mathbf{u}'\, d\mathbf{u}' \approx \mathbf{0}, \tag{44}$$

$$\overset{\leftrightarrow}{\mathbf{G}}_2(\mathbf{r}, \tau) = \int 3 \frac{\tilde{g}(\mathbf{r}, \mathbf{u}', \tau)}{4\pi \tilde{\ell}_s(\mathbf{r}, \mathbf{u}', \tau)} (\mathbf{u}' \otimes \mathbf{u}')\, d\mathbf{u}' \approx \frac{g(\mathbf{r})}{\ell_s(\mathbf{r})} \overset{\leftrightarrow}{\mathbf{I}}, \tag{45}$$

where $g(\mathbf{r})$ is $\tilde{g}(\mathbf{r}, \mathbf{u}', \tau)$ taken at $\tau = 0$, which, therefore, does not depend on $\mathbf{u}'$ anymore. The diffusion tensor can also be simplified in the form

$$\overset{\leftrightarrow}{\mathbf{D}}(\mathbf{r}, \tau) = \frac{v_E(\mathbf{r})}{3} \left[\frac{\overset{\leftrightarrow}{\mathbf{I}}}{\ell_e(\mathbf{r})} - \frac{g(\mathbf{r})}{\ell_s(\mathbf{r})} \overset{\leftrightarrow}{\mathbf{I}} \right]^{-1} \approx D(\mathbf{r}) \overset{\leftrightarrow}{\mathbf{I}}, \tag{46}$$

where, again making use of the weak absorption approximation, the diffusion constant is given by

$$D(\mathbf{r}) = \frac{v_E(\mathbf{r})\ell_t(\mathbf{r})}{3}, \tag{47}$$

with

$$\ell_t(\mathbf{r}) = \frac{\ell_s(\mathbf{r})}{1 - g(\mathbf{r})}, \tag{48}$$

the transport mean free path. We put forward that in this setting the effective absorption length remains unmodified and is given by

$$\frac{1}{\tilde{\ell}_a(\mathbf{r}, \tau)} = \frac{1}{\ell_e(\mathbf{r})} - M_0(\mathbf{r}, \tau)$$
$$= \frac{1}{\ell_e(\mathbf{r})} - \frac{\rho(\mathbf{r})}{4\pi} \int \sigma_s(a, \omega_0) p(a, \omega_0, \mathbf{u} \cdot \mathbf{u}')$$
$$\times e^{ik_r(\mathbf{u}'-\mathbf{u})\cdot\mathbf{v}\tau} f(\mathbf{r}, a, \mathbf{v})\, da\, d\mathbf{v}\, d\mathbf{u}\, d\mathbf{u}'. \tag{49}$$

In this formulation, the decorrelation M_0 appears as an extra contribution to the intrinsic absorption $1/\ell_a$.

With this expression of the effective absorption, the zero-order moment of the RTE [i.e., Eq. (27)] and the Fick's law [i.e., Eq. (39)] can be rewritten in the form

$$\nabla_{\mathbf{r}} \cdot \mathbf{q}_d(\mathbf{r}, \tau) = -\frac{v_E(\mathbf{r})}{\tilde{\ell}_a(\mathbf{r}, \tau)} u_d(\mathbf{r}, \tau) + \frac{I_b^-(\mathbf{r}, \tau) + I_b^+(\mathbf{r}, \tau)}{\ell_s(\mathbf{r})}, \tag{50}$$

$$\mathbf{q}_d(\mathbf{r}, \tau) = -D(\mathbf{r})\nabla_{\mathbf{r}} u_d(\mathbf{r}, \tau) + \frac{g(\mathbf{r})}{1 - g(\mathbf{r})}$$
$$\times \left[I_b^+(\mathbf{r}, \tau) - I_b^-(\mathbf{r}, \tau) \right] \mathbf{u}_z. \tag{51}$$

Combining Eqs. (50) and (51), we readily obtain the following diffusion equation for the diffuse energy density:

$$-\nabla_{\mathbf{r}} \cdot [D(\mathbf{r})\nabla_{\mathbf{r}} u_d(\mathbf{r}, \tau)] + \frac{v_E(\mathbf{r})}{\tilde{\ell}_a(\mathbf{r}, \tau)} u_d(\mathbf{r}, \tau) = S(\mathbf{r}, \tau), \tag{52}$$

with the source term

$$S(\mathbf{r}, \tau) = \frac{I_b^-(\mathbf{r}, \tau) + I_b^+(\mathbf{r}, \tau)}{\ell_s(\mathbf{r})} - \nabla_{\mathbf{r}} \left\{ \frac{g(\mathbf{r})}{1 - g(\mathbf{r})} \left[I_b^+(\mathbf{r}, \tau) - I_b^-(\mathbf{r}, \tau) \right] \right\} \mathbf{u}_z. \tag{53}$$

Equation (52) is the first important result of this work and deserves to be commented. First, the quasi-inhomogeneous aspect of the ejecta is encoded in the position dependence of the diffusion constant. Second, the dynamics of the particle cloud is taken into account in the τ dependence of the effective absorption mean free path. The standard diffusion equation is recovered in the absence of any $\mathbf{r}$ and τ dependence of $D(\mathbf{r})$ and $\tilde{\ell}_a(\mathbf{r}, \tau)$.

D. Geometry, boundary conditions, and source term

To complete this model, we need to determine the source term and the boundary conditions. To this end, we need to define the geometry used to represent the ejecta.

We consider a translation invariant (infinite) scattering slab along the transverse x and y directions, with length L along its longitudinal z-axis (see Fig. 4). This is a well-suited configuration for ejecta generated by a planar shock. The left-hand side interface of this slab, located at $z = z_l$, is assumed to be a reflective free surface traveling at velocity $v_s \mathbf{u}_z$. The right-hand side interface is an open interface located at $z = z_r$ and traveling at velocity $v_m \mathbf{u}_z$ (maximum cloud velocity). Since position $z = 0$ marks the initial position of the free surface and the particle cloud at $t = 0$, we have
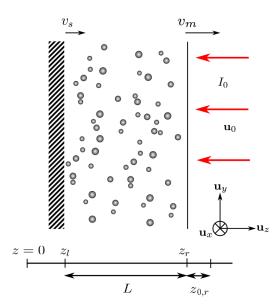
$$z_l = v_s t, \quad z_r = v_m t \quad \text{and} \quad L = (v_m - v_s)t. \tag{54}$$

This medium is illuminated by a plane wave with frequency ω_0 and intensity I_0 propagating along the direction $\mathbf{u}_0 = -\mathbf{u}_z$. This does not correspond to the real illumination of a standard ejecta experiment where an optical fiber is used but it has the advantage of preserving translational invariance along x and y. Considering perfect reflection at the free surface at position z_l, the ballistic intensities I_b^- and I_b^+ governed by Eq. (20) are given by

$$I_b^-(z, \tau) = I_0 \exp\left[-\int_z^{z_r} \frac{1}{\ell_e(z')}\, dz' \right], \tag{55}$$

$$I_b^+(z, \tau) = I_b^-(z_l) \exp(-2ik_r v_s \tau) \exp\left[-\int_{z_l}^z \frac{1}{\ell_e(z')}\, dz' \right]. \tag{56}$$

We note here that I_b^- does not decorrelate in time, and we can drop the τ dependency, while I_b^+ decorrelates due to the motion of

FIG. 4. Translation invariant and infinite along x-axis and y-axis scattering slab of length L along its longitudinal z-axis. This slab is illuminated from the right by a plane wave of intensity I_0 and frequency ω_0 propagating in the direction $\mathbf{u}_0 = -\mathbf{u}_z$. The front of the particle cloud is moving at velocity v_m and constitutes the right interface. The boundary condition for the diffuse energy density at this interface is given by the usual extrapolation length $z_{0,r} = (2/3)\ell_t(z_r)$. The left interface is the reflective free surface moving at velocity v_s. The position $z = 0$ marks the initial position of the free surface and the particle cloud at $t = 0$.

the free surface. Then, the source term of the diffusion equation becomes

$$S(z, \tau) = \frac{I_b^-(z) + I_b^+(z, \tau)}{\ell_s(z)} - \frac{\mathrm{d}}{\mathrm{d}z}\left\{\frac{g(z)}{1 - g(z)}\left[I_b^+(z, \tau) - I_b^-(z)\right]\right\}, \tag{57}$$

which finally leads to the diffusion equation

$$-\frac{\partial}{\partial z}\left[D(z)\frac{\partial}{\partial z}u_d(z, \tau)\right] + \frac{v_E(z)}{\overline{\ell}_a(z, \tau)}u_d(z, \tau) = S(z, \tau). \tag{58}$$

The final step concerns boundary conditions for the diffuse energy density u_d. Determining the relevant boundary conditions is not an easy task since u_d does not hold any information on direction. The problem can be tackled in different ways. One possibility consists in solving the Milne problem.[32,33] Here, we choose to stick to the P1 approximation,[14] which gives similar results.

Let us start with the boundary condition at the interface at $z = z_r$. The fact that there is no incoming diffuse light means that in terms of specific intensity

$$\int_{\mathbf{u}\cdot\mathbf{u}_z<0} I_d(z_r, \mathbf{u}, \tau)\mathbf{u}\cdot\mathbf{u}_z\,\mathrm{d}\mathbf{u} = 0. \tag{59}$$

Plugging in this expression the P1 approximation and noting that Eq. (51) becomes

$$\mathbf{q}_d(z, \tau)\cdot\mathbf{u}_z = -D(z)\frac{\partial}{\partial z}u_d(z, \tau) + \frac{g(z)}{1 - g(z)}\left[I_b^+(z, \tau) - I_b^-(z)\right] \tag{60}$$

in the slab geometry, we find that

$$u_d(z_r, \tau) + z_{0,r}\frac{\partial}{\partial z}u_d(z = z_r, \tau) = \frac{2g(z_r)\left[I_b^+(z_r, \tau) - I_b^-(z_r)\right]}{v_E(z_r)[1 - g(z_r)]}, \tag{61}$$

with $z_{0,r} = (2/3)\ell_t(z_r)$. We recover here the usual boundary condition for an open interface,[13,14] where $z_{0,r}$ is known as the extrapolation length.

Considering perfect reflection on the free surface at $z = z_l$, we find the relation

$$I_d(z_l, \mathbf{u}, \tau) = I_d[z_l, \mathbf{u} - 2(\mathbf{u}\cdot\mathbf{u}_z)\mathbf{u}_z, \tau]\exp[-2ik_rv_s(\mathbf{u}\cdot\mathbf{u}_z)\tau] \tag{62}$$

on the diffuse specific intensity for $\mathbf{u}\cdot\mathbf{u}_z > 0$. The first angular moment of the relation leads to an equality of the radiative flux given by

$$\int_{\mathbf{u}\cdot\mathbf{u}_z>0} I_d(z_l, \mathbf{u}, \tau)\mathbf{u}\cdot\mathbf{u}_z\,\mathrm{d}\mathbf{u} = -\int_{\mathbf{u}\cdot\mathbf{u}_z>0} I_d[z_l, \mathbf{u} - 2(\mathbf{u}\cdot\mathbf{u}_z)\mathbf{u}_z, \tau]$$
$$\times \exp[-2ik_rv_s(\mathbf{u}\cdot\mathbf{u}_z)\tau][\mathbf{u} - 2(\mathbf{u}\cdot\mathbf{u}_z)\mathbf{u}_z]\cdot\mathbf{u}_z\,\mathrm{d}\mathbf{u}. \tag{63}$$

Again, plugging the P1 approximation and making use of Eq. (60) leads to

$$-\left[\frac{1}{2} + \frac{3}{2}b(\tau)\right]\frac{\partial}{\partial z}u_d(z = z_l, \tau)$$
$$= -\left[\frac{1}{2} + \frac{3}{2}b(\tau)\right]\frac{g(z_l)}{D(z_l)[1 - g(z_l)]}\left[I_b^+(z_l) - I_b^-(z_l)\right]$$
$$+ \frac{v_E(z_l)}{D(z_l)}\left[\frac{1}{4} - \frac{a(\tau)}{2}\right]u_d(z_l, \tau), \tag{64}$$

where

$$a(\tau) = i\frac{1}{2k_rv_s\tau}\exp(-2ik_rv_s\tau)$$
$$- i\frac{1}{2k_rv_s\tau}\mathrm{sinc}(k_rv_s\tau)\exp(-ik_rv_s\tau), \tag{65}$$

$$b(\tau) = i\frac{1}{2k_rv_s\tau}\exp(-2ik_rv_s\tau) - i\frac{a(\tau)}{k_rv_s\tau}. \tag{66}$$

We note that when $\tau = 0$ or equivalently $v_s = 0$, we simply have $a = 1/2$ and $b = 1/3$. From Eq. (60), we find that $\mathbf{q}_d(z_l, \tau = 0)\cdot\mathbf{u}_z = 0$, which is consistent with the expected result for perfect reflection (no radiative flux).

E. Collected flux in reflection

In order to describe real PDV spectrograms using the diffusion equation, we first need to express the flux collected by a PDV probe as a function of the ballistic intensity I_b^+ and of the diffuse energy density.

In terms of the specific intensity, the flux collected by the probe is

$$\Phi_p(\tau) = S_p \left[I_b^+(z_r, \tau) + \int_{\theta_p} I_d(z_r, \mathbf{u}, \tau)(\mathbf{u} \cdot \mathbf{u}_z) \, d\mathbf{u} \right], \quad (67)$$

where S_p is the surface of the probe and θ_p is the angle of collection. Using the P1 approximation given by Eq. (26) and the definition of the numerical aperture $NA = n_r \sin \theta_p$, with n_r being the real part of the effective refractive index, the flux collected by the probe can be rewritten as

$$\Phi_p(\tau) = S_p I_b^+(z_r, \tau) + S_p \frac{v_E}{4} \frac{NA^2}{n_r^2} u_d(z_r, \tau)$$
$$+ S_p \frac{1}{2} \left[1 - \left(1 - \frac{NA^2}{n_r^2} \right)^{3/2} \right] [\mathbf{q}_d(z_r, \tau) \cdot \mathbf{u}_z]. \quad (68)$$

Using Eqs. (60) and (61) to write the flux as a function of the diffuse energy density, we obtain

$$\Phi_p(\tau) = S_p I_b^+(z_r, \tau)$$
$$+ S_p \frac{v_E}{4} \left\{ \frac{NA^2}{n_r^2} + \left[1 - \left(1 - \frac{NA^2}{n_r^2} \right)^{3/2} \right] \right\} u_d(z_r, \tau). \quad (69)$$

Since the specific intensity is assumed to be almost isotropic, we clearly see that the θ_p dependence of the collected flux factorizes. In the following, the expressions of both $\Phi_p(\tau)$ and the spectrogram $S(\Omega)$ will be useful. From Eqs. (4) and (15), we see that the expression of the spectrogram takes the form

$$S(\Omega) \propto \int \Phi_p(\tau) \cos(\Omega \tau) \, d\tau. \quad (70)$$

In this section, we have derived a diffusion equation relevant for the description of light propagation in ejecta, accounting for the statistical inhomogeneities and the motion of the scatterers. We have completed this model by adding appropriate boundary conditions and defining the collected flux. The next step is now to test the validity of the diffusion model against full RTE simulations, which is the objective of Sec. IV.

IV. POTENTIAL AND LIMITATION OF THE DIFFUSION MODEL

This section is dedicated to comparing the results obtained by a numerical resolution of the RTE and the solution of the diffusive model. The main idea is to start with a simple situation in which the physical parameters are chosen such that the solution of the diffusion approximation is expected to match the full numerical solution of the RTE. Then, one by one, we will increase the complexity by adding different ejecta characteristics to reach a situation corresponding to a real ejecta. This process will allow us to check step by step the validity of the diffusion model.

In the following, the numerical resolution of the RTE is performed using a Monte Carlo scheme, as presented in Ref. 10. Note that this scheme can be adapted to either compute the specific intensity in the τ-domain [i.e., $I(\mathbf{r}, \mathbf{u}, \tau)$] or in the ω-domain [i.e., $I(\mathbf{r}, \mathbf{u}, \omega)$] directly without requiring a Fourier transform, which is more computationally efficient. The diffusion model given by Eq. (58) together with the boundary conditions given by Eqs. (61) and (64) is solved using a finite-difference scheme. Once the diffuse energy density $u_d(z, \tau)$ has been computed, the flux collected by the probe, the spectrogram, and other derived quantities can be obtained directly. As an order of magnitude, the computation of a spectrogram using the Monte Carlo scheme requires about 1×10^8 photons and takes about 8 h on a computing cluster using 24 48-core Intel Xeon Gold 5220R, each clocked at 2.2 GHz, while the solution of the diffusion equation takes only 1 h on a regular laptop using a 4-core Intel Core i7-8665U CPU clocked at 1.90 GHz. This clearly illustrates the interest of using a diffusion model whenever it is relevant.

A. Statistically homogeneous medium with isotropic velocity distribution

We first consider the simple case of a statistically homogeneous particle cloud, the number density of which is given by

$$\rho = \frac{M_s}{m_p L}, \quad (71)$$

where M_s is the total ejected surface mass and $m_p = 4/3\pi \rho_{Sn} a_0^3$ is the mass of a single particle, with ρ_{Sn} being the volume density of tin. We recall that L is the cloud thickness (see Fig. 4). We also choose an isotropic Gaussian velocity distribution

$$j(\mathbf{v}) = \frac{1}{\sigma_v^2 (2\pi)^{3/2}} \exp \left(-\frac{|\mathbf{v}|^2}{2\sigma_v^2} \right). \quad (72)$$

We finally consider a mono disperse medium such that the particle size distribution is given by

$$h(a) = \delta(a - a_0), \quad (73)$$

where a_0 is the radius of the particles. In this setting, the size-velocity distribution is simply

$$f(z, a, \mathbf{v}) = h(a)j(\mathbf{v}). \quad (74)$$

Additionally, we neglect the role of the free surface and assume open boundary conditions at both z_l and z_r taking the form

$$u_d(z_l, \tau) - z_{0,l} \frac{\partial}{\partial z} u_d(z = z_l, \tau) = \frac{2g I_b^-(z_l)}{v_E(1 - g)}, \quad (75)$$

$$u_d(z_r, \tau) + z_{0,r} \frac{\partial}{\partial z} u_d(z = z_r, \tau) = -\frac{2g I_b^-(z_r)}{v_E(1-g)}, \tag{76}$$

with $z_{0,l} = z_{0,r} = (2/3)\ell_t$. We note that $I_b^+ = 0$ in the absence of the free surface.

Making $\tilde{\ell}_a$ given in Eq. (49) explicit using the velocity distribution given in Eq. (72) leads to

$$\frac{1}{\tilde{\ell}_a(\tau)} = \frac{1}{\ell_e} - \frac{2\pi}{\ell_s} \int \exp\left[-\sigma_v^2 k_r^2 \tau^2 (1-\mu)\right] p(a_0, \mu) \, d\mu, \tag{77}$$

where $\mu = \mathbf{u} \cdot \mathbf{u}'$. We see that at long correlation times, $\lim_{\tau \to +\infty} 1/\tilde{\ell}_a(\tau) = 1/\ell_e$. The integral over μ is computed numerically, and this configuration will be used as a reference in the following.

We first focus on the transmitted flux $\phi_t(\tau)$, since the diffusion equation is known to be more accurate in transmission. In the diffusion approximation, its expression is given by

$$\phi_t(\tau) = -\frac{v_E}{2} u_d(z_l, \tau) + I_b^-(z_l). \tag{78}$$

In practice, the ballistic component is negligible since the optical thickness is large. $\phi_t(\tau)$ is plotted in Fig. 5(a) and the corresponding spectrogram

$$S_t(\Omega) \propto \int \phi_t(\tau)(\cos \Omega \tau) \, d\tau \tag{79}$$

is plotted in Fig. 6(a) with the set of parameters $a_0 = 1 \, \mu m$, $M_s = 20 \, mg/cm^2$, $\sigma_v = 1000 \, m/s$, $v_s = 2250 \, m/s$, $v_m = 4500 \, m/s$, and $n_r = 1$. The plots are represented at time $t = 10 \, \mu s$ such that $L = 2.25 \, cm$. This corresponds to optical thicknesses $b_s = 45$ and $b_t = L/\ell_t = 23$. As a rule of thumb, we assume that $b_t > 10$ is needed for the diffusion approximation to be valid, which is largely satisfied here. Additionally, we have $g = 0.46$. As observed in Figs. 5(a) and 6(a), a good agreement is obtained between the RTE numerical computation and the diffusion model both in the time domain and in the frequency domain (spectrogram).

These results in a simple configuration and in transmission confirm, in particular, that the effective absorption term in the diffusion model correctly renders the decorrelation due to motion of the scatterers. They also confirm that it is not necessary to retain a τ dependency in the other parameters of the diffusion equation.

We now consider a situation in which the flux is collected in reflection by the probe ϕ_p, and the results are plotted in Figs. 5(b) and 6(b). We clearly see some important deviations especially at long correlation times and low frequencies. This discrepancy is due to a known limitation of the diffusion equation that it is much less accurate in reflection.[26] Indeed, in this geometry, short paths with few scattering events can have a strong impact and are not well accounted for in the diffusion approximation. More precisely, the diffusion approximation overestimates the weight of short paths and a solution for improvement is to reduce their weight. Since short paths decorrelate less than long paths, their influence is mostly visible at long correlation times τ. We, therefore, choose to simply use a second-order Taylor expansion of the effective absorption term

$1/\tilde{\ell}_a(\tau)$ in terms of τ, in order to increase the effect of the effective absorption term at large τ, without affecting the short correlation time behavior. To proceed, we use the expression

$$\frac{1}{\tilde{\ell}_a(\tau)} \approx \frac{1}{\ell_a} + \frac{1}{\ell_s} \sigma_v^2 k_r^2 \tau^2 (1-g). \tag{80}$$

In practice, single backscattering events happening exactly at $z = z_r$ have a null effective path length and are, therefore, not dealt with by the previous correction. To mitigate this artifact, the source term in Eq. (53) is replaced by a Dirac source term at z_s satisfying

$$\int_{z_s}^{z_{0,r}} \frac{dz}{\ell_t(z)} = 1, \tag{81}$$

such that

$$S(z, \tau) = I_0 \delta(z - z_s). \tag{82}$$

The results obtained with the diffusion equation modified with the effective absorption term in Eq. (80) and the modified source term in Eq. (81) are also plotted in Figs. 5(b) and 6(b). Clearly, a better agreement is obtained and we will use this improved diffusion model in the following.

B. Free-surface boundary condition

Having checked the validity of the diffusion model in an open geometry, we can now include the free surface by making use of the boundary condition given in Eq. (64). With this boundary condition, it is interesting to compute the reflected flux and compare the result with that obtained in the previous configuration with an open boundary and with the same set of parameters. Results are presented in Figs. 5(c) and 6(c). We clearly see that the free surface does not affect the reflected flux. This is a consequence of the large optical thickness of the ejecta considered here. Indeed, few photons propagate over the entire medium and reach the free surface. The presence of the free surface has a negligible impact on the results.

C. Size distribution and inhomogeneity in the number density

We now focus on the influence of the particle size distribution and of the inhomogeneity in the particle number density of the ejecta. We start by considering a truncated lognormal size distribution for the particle sizes given by

$$h(a) = \begin{cases} \frac{K}{a\sigma\sqrt{2\pi}} \exp\left[-\frac{\ln^2(a/a_0)}{2\sigma^2}\right], & \text{if } a \in [a_{min}, a_{max}], \\ 0, & \text{otherwise}, \end{cases} \tag{83}$$

where K is a normalization constant given by

$$K = 2 \left\{ \mathrm{erf}\left[\frac{\ln(a_{max}/a_0)}{\sigma\sqrt{2}}\right] - \mathrm{erf}\left[\frac{\ln(a_{min}/a_0)}{\sigma\sqrt{2}}\right] \right\}^{-1}, \tag{84}$$

with erf being the Gauss error function. Thus, the average particle mass is given by $m_p = (4/3)\pi \rho_{Sn} \int h(a) a^3 \, da$, where the integral over a is computed numerically.
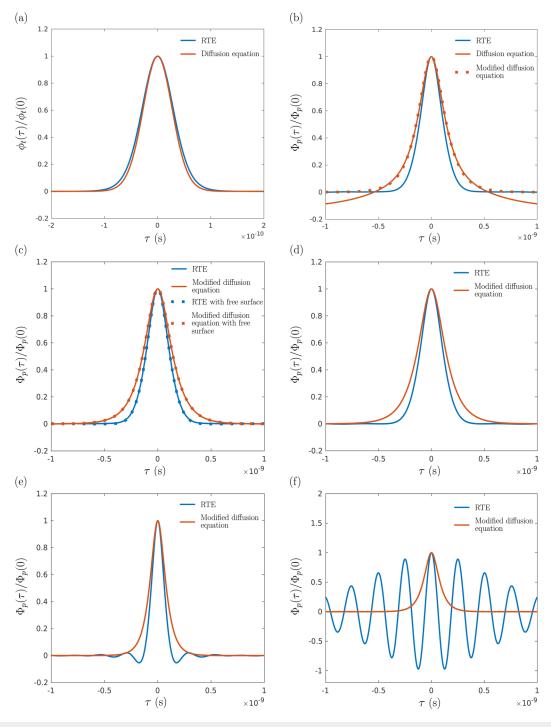
FIG. 5. Flux for different situations as a function of the correlation time τ. The RTE calculations are in blue, and the diffusion equation results are in red. (a) Total transmission for the statistically homogeneous medium with isotropic velocity distribution and open boundaries for both interfaces. (b) Same as (a) but for the flux collected by the probe in reflection. The computation using the modified effective absorption term in the diffusion equation is represented by a dotted line. (c) Same as (b) still with open boundaries (solid lines) or taking into account the free surface (dotted lines). (d) Same as (c) but with the free surface and a statistically homogeneous lognormal particle size distribution and an inhomogeneous particle number density. (e) Same as (d) but with an inhomogeneous isotropic velocity distribution. (f) Same as (e) but with an inhomogeneous anisotropic velocity distribution.

We also consider an inhomogeneous particle number density. This inhomogeneity in real ejecta is caused by the velocity difference between the slow particles at the back and the fast ones at the front, slow particles being more numerous. It is common to describe this inhomogeneity using mass-velocity distribution $M(v)$ taking the form of an exponential distribution.[34] Since we are considering a single shock in vacuum, we have $v = z/t$ for any particle. Therefore, $M(v)$ does depend on z/t directly and reads

$$M\left(\frac{z}{t}\right) = \begin{cases} M_s \exp\left(-\beta \frac{z}{v_s t}\right), & \text{if } z \in [z_l, z_r], \\ 0, & \text{otherwise,} \end{cases} \tag{85}$$

where M_s is the surface mass and the parameter β giving the slope of the distribution. The particle number density then takes the usual form

$$\rho(z) = \frac{\beta M(z/t)}{m_p v_s t}. \tag{86}$$

Note that $M(v)$ is used at this stage only to derive the expression of the inhomogeneous particle number density and does not affect the velocity distribution. Accounting for both the particle size distribution and the inhomogeneity in particle density, the effective absorption term takes the form

$$\frac{1}{\bar{\ell}_a(z, \tau)} = \frac{1}{\ell_a(z)} + \frac{1}{\ell_s(z)} \sigma_v^2 k_r^2 \tau^2 (1 - g). \tag{87}$$

The results are plotted in Figs. 5(d) and 6(d) for the same parameters as in the previous simulations and $\sigma = 0.5$, $a_0 = 0.66\,\mu m$, $a_{min} = 0.1\,\mu m$, $a_{max} = 2\,\mu m$, $M_s = 20\,mg/cm^2$, and $\beta = 10$. With these parameters, we solve for the optical thicknesses $b_s = 42$ and $b_t = \int 1/\ell_t(z)\,dz = 23$ and for the anisotropy factor $g = 0.47$.

We observe that the diffusion equation still gives accurate results compared to the RTE. In particular, position-dependent parameters in the diffusion model do not break its validity, providing that the optical thickness remains large enough for the diffusion approximation itself to be valid.

D. Fixed velocity modulus

In a single shock ejecta, at a given position, the particle velocity is known precisely. To improve the description of the ejecta and include this property, we shift from a homogeneous isotropic Gaussian velocity distribution to an inhomogeneous isotropic velocity distribution with fixed modulus. In terms of statistical distributions for the particle size and velocity, this means that we now take

$$f(z, a, \mathbf{v}) = h(a)j(z, \mathbf{v}), \tag{88}$$

$$j(z, \mathbf{v}) = \frac{1}{4\pi v_p^2(z)} \delta\left[|\mathbf{v}| - v_p(z)\right], \tag{89}$$

$$v_p(z) = v_s + \frac{z - v_s t}{L}(v_m - v_s). \tag{90}$$

In this setting, the effective absorption mean free path becomes

$$\frac{1}{\bar{\ell}_a(z, \tau)} = \frac{1}{\ell_e(z)} - 2\pi\rho(z) \int h(a)\sigma_s(a, \omega_0)p(a, \omega_0, \mu)$$
$$\times \text{sinc}\left[k_r\sqrt{2(1 - \mu)}v_p(z)\tau\right] da\,d\mu. \tag{91}$$

Performing the Taylor expansion near $\tau = 0$, this expression simplifies into

$$\frac{1}{\bar{\ell}_a(z, \tau)} = \frac{1}{\ell_a(z)} + \frac{1}{\ell_s(z)} \frac{v_p^2(z)}{3} k_r^2 \tau^2 (1 - g). \tag{92}$$

The results are plotted in Figs. 5(e) and 6(e) for the same parameters as in the previous simulations. We clearly observe a discrepancy between the full RTE calculation and the diffusion approximation. In particular, oscillations are visible for the RTE model in the τ-domain. These oscillations correspond to the single scattering contribution to Φ_p simply given by $\text{sinc}(\Omega_s\tau)$ in the simplified case $v_m = v_s$ (i.e., all particles have the same velocity). Since single scattering events are not well captured by the diffusion approximation, these oscillations are not visible in the diffusion model. This also leads to the appearance of a break in slope around $\Omega = 4k_r v_s$ for the spectrogram.

E. Anisotropic velocity

The last property to be included in order to model a realistic ejecta is the anisotropy in the particle velocity. Indeed, for a planar shock, the velocity must be along $\mathbf{u}_z$, the direction of ejection. This last condition is captured by a velocity distribution of the form

$$j(\mathbf{v}, z) = \delta\left[\mathbf{v} - v_p(z)\mathbf{u}_z\right]. \tag{93}$$

In these conditions, the effective absorption reads

$$\frac{1}{\bar{\ell}_a(z, \tau)} = \frac{1}{\ell_e(z)} - 2\pi\rho(z) \int h(a)\sigma_s(a, \omega_0)p(a, \omega_0, \mu) \tag{94}$$

$$\times \text{sinc}\left[k_r\sqrt{2(1 - \mu)}v_p(z)\tau\right] da\,d\mu, \tag{95}$$

which gives the following Taylor expansion around $\tau = 0$

$$\frac{1}{\bar{\ell}_a(z, \tau)} = \frac{1}{\ell_a(z)} + \frac{1}{\ell_s(z)} \frac{v_p^2(z)}{3} k_r^2 \tau^2 (1 - g). \tag{96}$$

We note that the angular velocity distribution has no effect on the effective absorption term since an integration is performed over all propagation directions $\mathbf{u}$ and $\mathbf{u}'$ in Eq. (49). In other words, the diffusion model is not sensitive to the velocity anisotropy.

The results are plotted in Figs. 5(f) and 6(f). While the diffusive model gives the same results, the RTE gives very different variations compared to the previous case. The reason is simple: the diffusion approximation is unable to take proper account of the angular distribution of velocities. However, the latter has a significant weighting in the low-order scattering events, which in turn
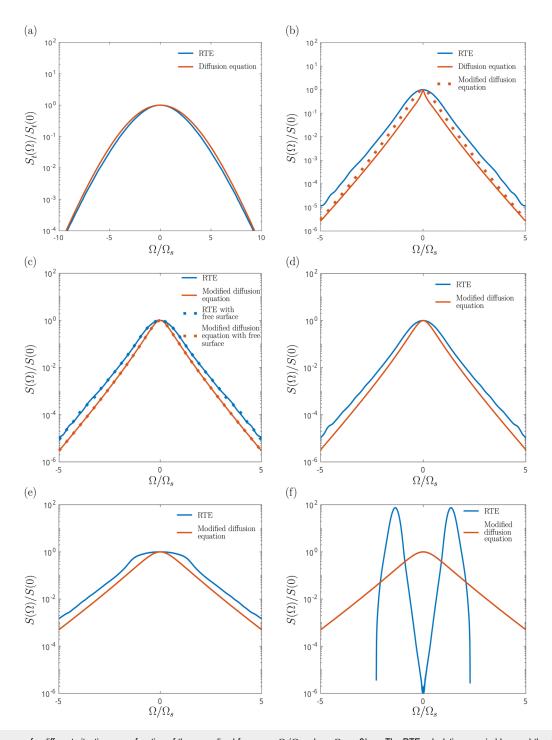
FIG. 6. Spectrogram for different situations as a function of the normalized frequency Ω/Ω_s, where $\Omega_s = 2k_r v_s$. The RTE calculations are in blue, and the diffusion equation results are in red. (a) Total transmission for the statistically homogeneous medium with isotropic velocity distribution and open boundaries for both interfaces. (b) Same as (a) but for the flux collected by the probe in reflection. The computation using the modified effective absorption term in the diffusion equation is represented by a dotted line. (c) Same as (b) still with open boundaries (solid lines) or taking into account the free surface (dotted lines). (d) Same as (c) but with the free surface and a statistically homogeneous lognormal particle size distribution and an inhomogeneous particle number density. (e) Same as (d) but with an inhomogeneous isotropic velocity distribution. (f) Same as (e) but with an inhomogeneous anisotropic velocity distribution.

have a significant weighting in the reflection spectrogram. The diffusive model is, thus, unable to predict the correct behavior of the spectrogram in situations in which the anisotropy in the velocity distribution is substantial.

V. CONCLUSION

In summary, we have derived a model that describes light transport in dynamic media in the diffusive regime (i.e., where the transport optical thickness is large). We have shown how a model based on the diffusion approximation and accounting for the specificities of an ejecta can be derived. This model gives valuable results compared to the RTE in many scenarios ranging from a statistically homogeneous and isotropic medium to an ejecta like configuration, in terms of both field–field time correlation function and spectrograms. At last, we have seen that the model fails to recover the results from the RTE for an isotropic velocity distribution with fixed modulus or even worse when the anisotropy of the ejecta velocity distribution cannot be neglected. This is a typical bias of the diffusion approximation, which assumes isotropic properties of the medium and light propagation. For standard planar shocks, the RTE, therefore, remains the reference model.

Nonetheless, while we have centered this work around planar shocks, the diffusion model showed to be very useful in scenarios where the ejecta has a quasi-spherical symmetry. This geometry applies, for instance, to the remarkably interesting work of Saunders *et al.* in Ref. 35 where the interaction of two microjets produces a non-planar ejecta. Additionally, a significant advantage of the diffusion model is its low computational cost compared to the RTE. This makes it a potentially useful tool for the analysis of PDV spectrograms in practical applications.

Finally, we believe that the idea of developing a simpler transport theory for light propagation in ejecta remains relevant and potentially useful in a broad range of practical applications. Approaches based on Delta-Eddington phase functions or a Fokker-Plank form of the RTE[13,36] are possibles lines to follow in future works.

ACKNOWLEDGMENTS

AUTHOR DECLARATIONS

Conflict of Interest

The authors have no conflicts to disclose.

Author Contributions

J. A. Don Jayamanne: Data curation (equal); Formal analysis (equal); Investigation (equal); Software (equal); Visualization (equal); Writing – original draft (equal). **J.-R. Burie:** Funding acquisition (equal); Supervision (equal); Writing – review & editing (equal). **O. Durand:** Writing – review & editing (equal). **R. Pierrat:** Conceptualization (equal); Supervision (equal); Validation (equal); Visualization (equal); Writing – review & editing (equal). **R. Carminati:** Conceptualization (equal); Funding acquisition (equal); Project administration (equal); Supervision (equal); Writing – review & editing (equal).

DATA AVAILABILITY

The data that support the findings of this study are available from the corresponding author upon reasonable request.

REFERENCES

[1]M. B. Zellner, G. Dimonte, T. C. Germann, J. E. Hammerberg, P. A. Rigg, G. D. Stevens, W. D. Turley, W. T. Buttler, M. Elert, M. D. Furnish, W. W. Anderson, W. G. Proud, and W. T. Butler, AIP Conf. Proc. **1195**, 1047–1050 (2009).

[2]T. de Rességuier, E. Lescoute, A. Sollier, G. Prudhomme, and P. Mercier, "Microjetting from grooved surfaces in metallic samples subjected to laser driven shocks," J. Appl. Phys. **115**, 043525 (2014).

[3]J. R. Asay, L. P. Mix, and F. C. Perry, "Ejection of material from shocked surfaces," Appl. Phys. Lett. **29**, 284–287 (1976).

[4]P. Andriot, P. Chapron, and F. Olive, "Ejection of material from shocked surfaces of tin, tantalum and lead-alloys," AIP Conf. Proc. **78**, 505–509 (1982).

[5]W. T. Buttler, R. J. R. Williams, and F. M. Najjar, "Foreword to the special issue on ejecta," J. Dyn. Behav. Mater. **3**, 151–155 (2017).

[6]R. D. Richtmyer, "Taylor instability in shock acceleration of compressible fluids," Commun. Pure Appl. Math. **13**, 297–319 (1960).

[7]E. E. Meshkov, "Instability of the interface of two gases accelerated by a shock wave," Fluid Dyn. **4**, 101–104 (1969).

[8]O. T. Strand, D. R. Goosman, C. Martinez, T. L. Whitworth, and W. W. Kuhlow, "Compact system for high-speed velocimetry using heterodyne techniques," Rev. Sci. Instrum. **77**, 083108 (2006).

[9]P. Mercier, J. Benier, A. Azzolina, J. M. Lagrange, and D. Partouche, "Photonic doppler velocimetry in shock physics experiments," J. Phys. IV **134**, 805–812 (2006).

[10]J. A. Don Jayamanne, J.-R. Burie, O. Durand, R. Pierrat, and R. Carminati, "Characterization of ejecta in shock experiments with multiple light scattering," J. Appl. Phys. **135**, 073105 (2024).

[11]J. A. Don Jayamanne, R. Outerovitch, F. Ballanger, J. Bénier, E. Blanco, C. Chauvin, P. Hereil, J. Tailleur, O. Durand, R. Pierrat, R. Carminati, A. Hervouët, P. Gandeboeuf, and J.-R. Burie, "Recovering particle velocity and size distributions in ejecta with photon Doppler velocimetry," J. Appl. Phys. **136**, 083111 (2024).

[12]S. Chandrasekhar, *Radiative Transfer* (Dover, New York, 1950).

[13]R. Carminati and J. C. Schotland, *Principles of Scattering and Transport of Light* (Cambridge University Press, 2021).

[14]A. Ishimaru, *Wave Propagation and Scattering in Random Media* (IEEE Press, 1997).

[15]Y. N. Barabanenkov, "On the spectral theory of radiation transport equations," Sov. Phys. JETP **29**, 679–684 (1969).

[16]S. M. Rytov, Y. A. Kravtsov, and V. I. Tatarskii, *Principles of Statistical Radiophysics* (Springer-Verlag, Berlin, 1989), Vol. 4.

[17]L. A. Apresyan, and J. A. Kravtsov, *Radiation Transfer: Statistical and Wave Aspects* (Gordon & Breach, Amsterdam, 1996).

[18]R. Elaloufi, R. Carminati, and J.-J. Greffet, "Definition of the diffusion coefficient in scattering and absorbing media," J. Opt. Soc. Am. A **20**, 678 (2003).

[19]R. Pierrat, J.-J. Greffet, and R. Carminati, "Photon diffusion coefficient in scattering and absorbing media," J. Opt. Soc. Am. A **23**, 1106 (2006).

[20]E. W. Larsen and J. B. Keller, "Asymptotic solution of neutron transport problems for small mean free paths," J. Math. Phys. **15**, 75–81 (1974).

[21]K. Furutsu and Y. Yamada, "Diffusion approximation for a dissipative random medium and the applications," Phys. Rev. E **50**, 3634–3640 (1994).

[22]T. Durduran, A. G. Yodh, B. Chance, and D. A. Boas, "Does the photon-diffusion coefficient depend on absorption? J. Opt. Soc. Am. A **14**, 3358 (1997).

[23]D. Pine, D. Weitz, J. Zhu, and E. Herbolzheimer, "Diffusing-wave spectroscopy: Dynamic light scattering in the multiple scattering limit," J. Phys. Fr. **51**, 2101–2127 (1990).

[24]B. J. Berne and R. Pecora, *Dynamic Light Scattering: With Applications to Chemistry, Biology, and Physics* (Dover Publications, Mineola, 2000).

[25]F. Scheffold, S. E. Skipetrov, S. Romer, and P. Schurtenberger, "Diffusing-wave spectroscopy of nonergodic media," Phys. Rev. E **63**, 061404 (2001).

[26]R. Pierrat, N. B. Braham, L. Rojas-Ochoa, R. Carminati, and F. Scheffold, "The influence of the scattering anisotropy parameter on diffuse reflection of light," Opt. Commun. **281**, 18–22 (2008).

[27]R. Pierrat, "Transport equation for the time correlation function of scattered field in dynamic turbid media," J. Opt. Soc. Am. A **25**, 2840 (2008).

[28]J. Harden and V. Viasnoff, "Recent advances in DWS-based micro-rheology," Curr. Opin. Colloid Interface Sci. **6**, 438–445 (2001).

[29]G. Labeyrie, R. Kaiser, and D. Delande, "Radiation trapping in a cold atomic gas," Appl. Phys. B **81**, 1001–1008 (2005).

[30]A. D. Klose and E. W. Larsen, "Light transport in biological tissue based on the simplified spherical harmonics equations," J. Comput. Phys. **220**, 441–470 (2006).

[31]J. A. Don Jayamanne, J. R. Burie, O. Durand, R. Pierrat, and R. Carminati, AIP Conf. Proc. **3066**, 610001 (2024).

[32]E. A. Milne, "Radiative equilibrium in the outer layers of a star: The temperature distribution and the law of darkening," Mon. Not. R. Astron. Soc. **81**, 361–375 (1921).

[33]K. Case, "Elementary solutions of the transport equation and their applications," Ann. Phys. **9**, 1–23 (1960).

[34]S. K. Monfared, D. M. Oró, M. Grover, J. E. Hammerberg, B. M. LaLone, C. L. Pack, M. M. Schauer, G. D. Stevens, J. B. Stone, W. D. Turley, and W. T. Buttler, "Experimental observations on the links between surface perturbation parameters and shock-induced mass ejection," J. Appl. Phys. **116**, 063504 (2014).

[35]A. Saunders, C. Stan, K. Mackay, B. Morgan, J. Horwitz, S. Ali, H. Rinderknecht, T. Haxhimali, Y. Ping, F. Najjar, J. Eggert, and H.-S. Park, "Experimental observations of laser-driven tin ejecta microjet interactions," Phys. Rev. Lett. **127**, 155002 (2021).

[36]P. González-Rodríguez and A. D. Kim, "Comparison of light scattering models for diffuse optical tomography," Opt. Express **17**, 8756 (2009).

05 December 2025 08:18:02